New Super-twisting Sliding Mode Control of an Upper Limb Rehabilitation Robot Based on the TLBO Algorithm

Naghmeh Mirrashid[1], EsmailAlibeiki[1*], Seyed Mehdi Rakhtala[2]

Abstract-Rehabilitation robots are very popular because they are beneficial tools in helping stroke patients and people with physical disabilities, so controlling them to get accurate performance is necessary. This paper presents a new super-twisting controller based on the determined gain with the TLBO algorithm (STA-TLBO) for an upper limb rehabilitation robot for the first time. One of the most important parts of designing the super twisting algorithm (STA) controller is determining the gains, which requires accurate calculations and obtaining disturbance. In this paper, the Teaching–Learning-Based Optimization (TLBO) algorithm is used to obtain the gains of the STA controller. To illustrate the validity of the proposed controller, the results are compared to PID, STA, and PID-TLBO controllers. The results indicate that the proposed controller ensures accurate tracking, finite-time convergence, and reduced chattering. The stability and the robustness of the PID-TLBO and STA-TLBO controllers are examined by three tests, parameter uncertainties, external disturbances, and step response. The results show that the STA-TLBO controller has a better performance than the others under different conditions; that means the proposed controller has a shorter convergence time, more accurate tracking, and fewer tracking error than the other three controllers.

Keywords: Rehabilitation robot, Dynamic modeling, Super twisting algorithm, TLBO algorithm, Lyapunov stability.

1. Introduction

Stroke, old age, and genetic diseases may cause weakness and disability of some organs of the body such as arms, legs and, etc. The mentioned patients need rehabilitation therapy to overcome such disabilities. The popularity of rehabilitation robots is due to the help of stroke patients and patients who suffer from muscle weaknesses because of congenital reasons [1]. Problems such as high volume, heavyweight, and large inertia, make it impossible for the patient to use a robot with a rigid mechanical structure alone. Compared to rigid exoskeletons, wearable exoskeletons are lightweight, more comfortable, smaller, and utilize human joints to rotate [2, 3]. The wearable rehabilitation robots are used in cases where the disability is less and the patient is not completely paralyzed [4, 5]. In recent years, many researchers have developed different types of wearable exoskeleton robots, which are comfortable, compliant, and low-cost [6].

The early robotic exoskeletons for upper limb rehabilitation are not complicated in hardware structure and design. Some researchers have remodeled, redesigned the upper limb robots to build a new version of them. For example, Tobias Nef et al. have introduced a rigid exoskeleton; so called the ARMin[7]. They also developed it in [8, 9]. Otten et al. have developed the powered exoskeleton DAMPACE [10] that can be used to identify the reflex properties of stroke patients which can be applied to rehabilitationtraining [11]. Keller et al. (2016) have proposed an exoskeleton with an

1 Department of Electrical Engineering, Aliabad Katoul Branch, Islamic Azad University, Aliabad Katoul, Iran. E-Mail: n.mirrashid@aliabadiau.ac.ir

1*Corresponding Author: Department of Electrical Engineering, Aliabad Katoul Branch, Islamic Azad University, Aliabad Katoul, Iran. E-Mail esmail_alibeiki@aliabadiau.ac.ir

2 Faculty of Engineering, Department of Electrical Engineering, Golestan University, Gorgan, Iran.E-Mail: sm.rakhtala@gu.ac.ir.

Received: 2022.09.28, Accepted: 2022.11.09

audiovisual therapy interface for the upper limb rehabilitation of adolescents and children and called ChARMin[12]. Also, an exoskeleton for superior extremity training, ETS-MARSE, has been introduced by [13]. Many other exoskeletons have been developed for upper limb rehabilitation that had heavyweight and have high energy consumption and a large structure. For overcoming these problems some methods have been introduced, and due to more complexity exoskeleton structure, and slight system reliability are not interested [14, 15]. Thus researchers have more focused on the wearable exoskeleton robots in which the force directly applies to the human skeleton [5, 16].

In general, the rehabilitation robot model is obtained using energy equations and Lagrange's relationships [17]. The human upper limb includes 7degrees of freedom (DOF): shoulder vertical and horizontal flexion/extension, shoulder internal/external rotation, elbow flexion/extension, forearm pronation/supination, wrist flexion/extension, and wrist radial/ulnar deviation . The models are considered based on their DOF.TianFuXiang[18] and Agrawal[19] have extended the parametric mass model of the Kaneko et al. [17]that described the transmission of tendon traction, but their development method was very complicated. The backlash-induced hysteresis in the motion control of a robotic upper limb modeling is an interesting issue and has been investigated by [20]. The Hill-based Muscle-Tendon Model is one of the most popular models for modeling the mechanical characteristics of muscle [5, 21].

The development of a control strategy to help accurately tracking is one of the greatest challenges in the control of robots. Crea et al. have presented a new external skeleton for upper limb power. They used a PID closed-loop controller to adjust the location of the joint that minimizes the error between the desired angle and the measured angle [22]. Kawasaki et al. used the PD controller to control the rehabilitation robot with 18 degrees of freedom. The controller of the proposed engine moves 22 servo motors in the manual motor robot. This system has two functions, the first one is to measure the angles of the healthy hand, and the second one is to control the backward joint angles with the time of sampling time that the sampling time is equal to 1ms [23]. Similarly, [24] and [25] have used the PID controller to control the rehabilitation robot performance. Li et al. have presented a new control method, including a repeated time-delayed neural network (TDRNN), to predict the kinematics of the upper limb and wrist robot with 3 DOF. Their proposed control method is considered the previous prediction of joint angles and SEMG signals as the system input and is used a batch training based on the Levenberg-Marquardt algorithm (LM) [26]. Kiguchi et al. have suggested a hierarchical neuro-fuzzy controller for an upper-limb robot exoskeleton, which consists of three steps: input signal selection, deployment area selection, and neuro-fuzzy control. This controller uses skin surface EMG signals as controller input signals [27]. Wu et al. have introduced a fuzzy sliding mode acceptance controller (FSMCA) for multi-mode elbow rehabilitation. The proposed controller shows high accuracy in tracking the path in the experimental mode and can be used for patients with different levels of weakness [5].

Kang and Wang have designed an adaptive robust output feedback controller for helping to shoulder joint movements, elbows, and wrists. Their controller is robust to uncertainty and disturbances [28]. Since with the change of the patient, the parameters of the model change too, so the system behavior will very nonlinear; the sliding mode controller can ensure consistency against the uncertainty of parameters and external disturbances [29]. Lily et al. (2004) developed a sliding mode controller to track upper limb movement. The tracking performance of the designed controller was accurate [30]. The authors in [31] have compared the performance of a nonlinear sliding mode controller to a PID controller in terms of tracking accuracy and have concluded that the performance of a nonlinear controller is better than a linear controller. Rahman et al., also, have used this method to control robots with 5 and 7 DOF [29, 32]. Joo et al. (2017) have used an adaptive sliding mode controller to control an upper limb robot and have achieved results including robust against external disturbances and parametric uncertainty [33]. Other applications of sliding mode controller can be found in [34, 35].

In 2011, Rao et al. have introduced the TLBO Algorithm [36], based on the traditional teaching method and the teacher's impact on students' learning. The introduced optimization algorithm is one of the modern successful algorithms in various fields and has good convergence speed and search accuracy [26, 37, 38]. Now, by considering the mentioned literature review, the contribution of the paper is to develop an STA controller to control the tracking performance of an upper limb rehabilitation robot, by considering the stability of the proposed controller.

The rest of the paper is organized as follows. Section 2 is devoted to the dynamic modeling of a rehabilitation robot. In section 3, the controller is designed. Section 4 explains the TLBO algorithm. The simulation results are given in Section 5. Finally, section 6 concludes the paper.

2. System modeling

To obtain the dynamic equations of the upper limb rehabilitation robot, we use the energy equations and the Euler-Lagrange method [39].

$$K(\beta(t),\dot{\beta}(t)) = \frac{1}{2}m||v||^2 + \frac{1}{2}I\beta^2 \quad (1)$$

$$L(\beta(t),\dot{\beta}(t)) = K(\beta(t),\dot{\beta}(t)) - U(\beta(t)) \quad (2)$$

$$\frac{d}{dt}\left(\frac{\partial L(\beta,\dot{\beta})}{\partial \dot{\beta}}\right) - \frac{\partial L(\beta,\dot{\beta})}{\partial \beta} = \tau \quad (3)$$

Where K is kinetic energy, β is a joint position, $\dot{\beta}$ is time derivative of the position, m is the mass, v is the angular velocity vector, I is the inertia, L is lagrangian, U is potential energy and τ represents the driving torque from the servo motor.

Fig. 1 shows the structure of an upper limb robot.

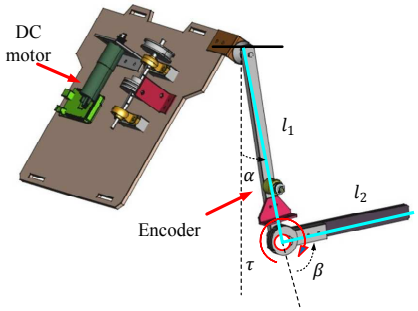

Fig. 1. Structure of an upper limb robot [40].

It can be written by considering the position vector of the center of mass from each link [41]:

$$P = \begin{bmatrix} l_1 sin(\alpha) + l_2 sin(\alpha+\beta) \\ -l_1 cos(\alpha) - l_2 cos(\alpha+\beta) \end{bmatrix}$$

whereP is a position vector, α is a constant angle and $\beta \in R$ is the position angle for the vertical axis, l_1 and l_2 are the lengths of link 1 and link 2, respectively. According to relations (1)- (3), we have:

$$(m_2 l_2^2)\ddot{\beta} + m_2 l_2 g sin(\alpha+\beta) = \tau - F_{ext}(\beta,\dot{\beta},t) \quad (4)$$

whereFext(β,$\dot{\beta}$,t)∈R is external forces as friction or disturbances ,and can be expressed as:

$$F_{ext} = F_c sign(\dot{\theta}) - F_v\dot{\theta} \quad (5)$$

whereF_c is the coulomb-friction constant and F_v is the viscous friction coefficient. On the other hand, the actuator dynamics are equal to:

$$J_m\ddot{\beta} + \frac{1}{r}f_m(r\dot{\beta}) + \frac{K_aK_b}{R_a}\dot{\beta} + \frac{\tau}{r^2} = \frac{K_a}{rR_a}v, \quad 6)$$

where J_m, $f_m(r\dot{\beta})$,K_a, K_b,R_a, r, and v(t) are, respectively, the inertia of the rotor, the friction between the rotor and its bearing, the motor-torque constant, the back emf constant, the armature resistance, the gears reduction ratio, the armature voltage and control input. Thus, the dynamic model of rehabilitation upper limb robot will equal to:

$$\left[\frac{1}{r^2}(m_2 l_2^2 + I_2) + J_m\right]\ddot{\beta} + \frac{1}{r}f_m(r\dot{\beta}) + \frac{m_2 l_2 g}{r^2}sin(\alpha+\beta) + \left[\frac{K_aK_b}{R_a} + \frac{F_v}{r^2}\right]\dot{\beta} + \frac{F_c}{r^2}sign(\dot{\beta}) = \frac{K_a}{rR_a}v \quad (7)$$

The parameters of the system are given in Table.1.

Table.1. The parameter values of the robot model[42]

Parameter of the robot model	Values
m_2	0.1 kg
l_2	0.4 m
g	9.8 m/s^2
Armature Resistance R_a	0.56 Ω
Inertia Constant J_m	$0.083Nm/(rad/s^2)$
Gears reduction ratio r	0.01
Motor-torque constant K_a	$0.43\ V/(rad/sec)$
Back emf Constant K_b	$0.43\ V/(rad/sec)$
Armature Current i_a	0.2639 A

3. Design and analysis of super twisting controller

We can define the sliding surface s(t) by considering the tracking error as $e = \beta_d - \beta$ (β_d is the desired trajectory for joint) as follows:

$$s(t) = k_p e(t) + k_d\dot{e}(t) + \gamma e^{\mu} \quad (8)$$

wherek_p ,k_d, γ, and μ are positive constants. The super twisting algorithm can be written by [43]:

$$U = u_1 + u_2 \quad (9)$$

$$u_1 = -k_1|s|^{\frac{1}{2}}sign(s)$$

$$\dot{u}_2 = -k_2 sign(s).$$

where$k_1$and $k_2$are controller coefficients. The quadratic form of Lyapunov's function is:

$$V_Q(s) = z^T P z \quad (10)$$

$$A^T P + PA = -Q, \quad (11)$$

Where$z^T = \Phi^T(s) = [\phi_1(s), u_2]$, in which P is a unique positive definite symmetric matrix, $\phi_1(s) = |s|^{\frac{1}{2}}sign(s)$, $\phi_2(s) = sign(s)$, $A = \begin{bmatrix} -k_1 & 1 \\ -k_2 & 0 \end{bmatrix}$ and $Q = Q^T > 0$ is a positive definite matrix.

One can write $\phi_2(s) = \phi'_1(s)\phi_1(s)$, and $\phi'_1(s) = \frac{1}{2}|s|^{-\frac{1}{2}}$. Thus

$$\dot{z} = \begin{bmatrix} \phi'_1(s)\{-k_1\phi_1(s) + s\} \\ -k_2\phi_2(s) \end{bmatrix} = \phi'_1(s)\begin{bmatrix} -k_1 & ,1 \\ -k_2 & ,0 \end{bmatrix}\zeta = \phi'_1(s)Az \quad (12)$$

And the derivative of the Lyapunov function is:

$$\dot{V}_Q(s) = \dot{z}^T Pz + z^T P\dot{z} = \phi'_1(s)z^T(A^T P + PA)z = -\phi'_1(s)z^T Qz \quad (13)$$

where Q can be calculated from the equation ALE (11). We had standard inequality for quadratic forms:

$$\lambda_{\min}\{P\}\|z\|_2^2 \le z^T Pz \le \lambda_{\max}\{P\}\|z\|_2^2$$

where $\|z\|_2^2 = \phi_1^2(s) + u_2^2 = |s| + u_2^2$, and note that the inequality $|s|^{-\frac{1}{2}} \le |\phi_1(s)| \le \|z\|_2 \le \frac{V_Q^{\frac{1}{2}}(s)}{\lambda_{\min}^{\frac{1}{2}}\{P\}}$ holds.

Therefore $-|s|^{-\frac{1}{2}} \le -\frac{V_Q^{\frac{1}{2}}(s)}{\lambda_{\min}^{\frac{1}{2}}\{P\}}$. This shows that

$$\dot{V}_Q \le -\lambda_{\min}\{Q\}\phi'_1(s)\|z\|_2^2 \quad (14)$$

$$\dot{V}_Q \le -\lambda_{\min}\{Q\}\left(\frac{1}{2}|s|^{-\frac{1}{2}}\right)\|z\|_2^2 \le -\frac{\frac{1}{2}\lambda_{\min}\{Q\}\left(\lambda_{\min}^{\frac{1}{2}}\{P\}\right)^{-1}}{\lambda_{\max}\{P\}}V_Q^{\frac{1}{2}}(s)$$

Therefore V_Q decreases uniformly and has a stable asymptotic origin. This indicates that V_Q is a strong Lyapunov function. On the other hand the answer to the differential equation $\dot{v} = -\gamma_1 v^{\frac{1}{2}}$, $v(0) = v_0 \ge 0$ is equal to

$$v(t) = \left(v_0^{\frac{-1}{2}} - \frac{1}{2}\gamma_1 t\right)^{-2}, \quad \gamma_1 > 0 \quad (15)$$

Therefore, the convergence time can be estimated as follows:

$$T(x_0) = \frac{1}{\frac{-1}{2}\gamma_1(Q)}V_Q^{\frac{1}{2}}(x_0) \quad (16)$$

To ensure finite-time convergence and to establish Lyapunov stability conditions, the controller coefficients must have determined as follows [43, 44]:

$$k_1^2 \ge \frac{4\ c\ k_M(k_2 + c)}{k_m^3(k_2 - c)},\ k_2 > \frac{c}{k_m} \quad (17)$$

where for all $u \in U$ and$x \in X$,$|\frac{\delta}{\delta x}s| \le c$, $0 < k_m < \frac{\delta}{\delta x}\dot{s} < k_M$.

4. TLBO Optimization

In this paper, the TLBO algorithm is applied to find the optimal values of the controller coefficient. TLBO algorithm has two stages: the teacher's influence on students and the student's influence on each other. The algorithm, first, selects a population of students randomly, then the best member of the selected population is considered as a teacher. The teacher tries to improve the knowledge level of his (her) class. To improve the class knowledge level, the algorithm calculates the difference between the teacher's knowledge and the average of all students and improves the knowledge of other students to the level of the teacher. Each student is given a commensurate rank with his or her level of knowledge, and at the end of each round of repetition of the teaching process, the best member of the population is recognized as the teacher who will share their knowledge with other members of the population. Students try to get a better grade than their previous status based on the academic status of their classmates and the quality of teacher education. The parameters of the algorithm include the number of learners (nL) and the maximum number of target performance evaluations.

The flowchart of TLBO algorithm is presented in Fig. 2. In general, the algorithm can be summarized as follows [36, 38]:

1- New learners (Np) are trained based on the teacher level. The population can be given as follows:

$$Pop = \begin{bmatrix} x_{1,1} & x_{1,2} & \dots & x_{1,d} \\ \vdots & \vdots & \ddots & \vdots \\ x_{Np} & x_{Np,2} & \dots & x_{Np,d} \end{bmatrix},$$

whereNp is population size, and d is number of design variables.

2- By calculating the average values of scores of students, the performance of the whole class is obtained.

$$Mean_P = [mean_1 \quad mean_2 \quad \dots \quad mean_d]$$

3- The TLBO algorithm promotes students by the difference between the teacher's position ($x_{teacher}$) and the average position of all students in the random composition ($Mean_P$). That means:

$$X_{new} = X_{old} + r(x_{teacher} - (T_f)Mean_{P,new}),$$

where r and T_f are random number on interval [0,1] and teaching factor, respectively.

4- At this stage, either new learners (Np) are created or students' knowledge is updated through interaction with each other in the learning stage. Each student (X_i) is compared to another randomly selected student (X_{rp}). If the student has better knowledge ($PFit_i$<$PFit_{rp}$), then

he (she) is transferred to the selected student position;

$X_{new} = X_{old} + r(X_{rp} - X_i)$,

otherwise relocates

$X_{new} = X_{old} + r(X_i - X_{rp})$.

In the learning phase, each person tries to make progress by sharing their information with a randomly selected person.

5- Finally, the algorithm improves as the difference between students' knowledge decreases, and the size of the search step gradually decreases, and this completes the algorithm.

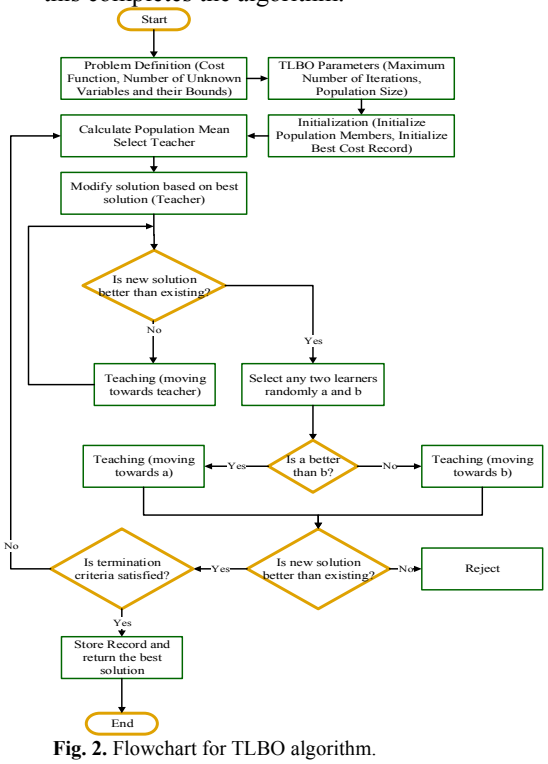

Fig. 2. Flowchart for TLBO algorithm.

The objective function (O_F) is defined according to the motion trajectory error of joints is O_F=$\sqrt{\int_0^\infty |e(t)|^2 dt}$, where $e(t) = \beta_d - \beta$.

5. Results and discussion

5.1. PID-TLBO controller

In The PID controller coefficients are adjusted using the TLBO algorithm.

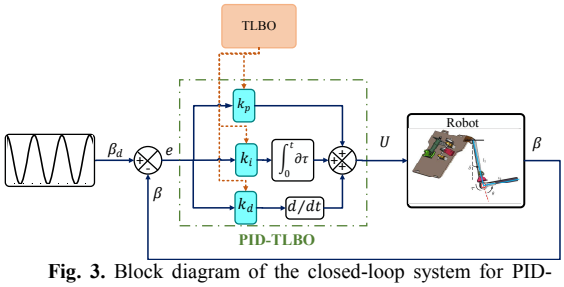

Fig. 3. Block diagram of the closed-loop system for PID-TLBO.

Fig. 3 shows the block diagram of the closed-loop system for PID-TLBO. The relationship for the desired path of tracking is given as follows.

$$\beta_d = sin(2\pi ft) + 1 \quad (18)$$

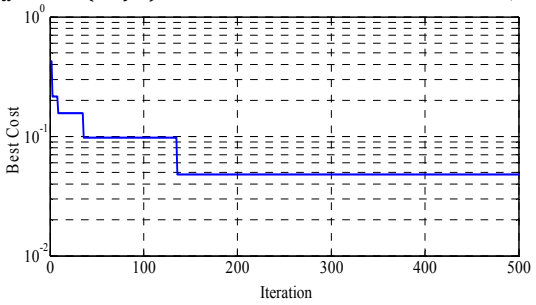

Fig. 4. The convergence rate for PID-TLBO objective function.

The convergence rate for the PID-TLBO objective function with the best value of 0.04786 in the 136th iteration shows in Fig. 4.

5.2. STA-TLBO controller

In general, the coefficients of the STA controller are calculated from equation (9) by obtaining the perturbation bounds that is a time-consuming process. The intelligent TLBO algorithm simplifies the adjustment of the STA controller coefficients and provides acceptable results.

Fig. 5 and Fig. 6 show the block diagram of the closed-loop system and the best objective function with the best value of 0.0075 in the 557th iteration, respectively.

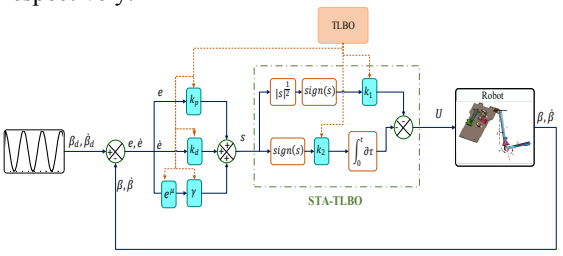

Fig. 5. Block diagram of the closed-loop system for STA-TLBO.

Table 2. shows the parameters of controllers.

Table 2. The Controllers parameters.

	k_p	k_i	k_d	γ	μ
PID	8029.9	18.979	30.59	-	-
STA	200	30	-	800	5
PID-TLBO	90.936	35.141	25.52	-	-
STA-TLBO	381.47	48.1158	-	876.45	2.03

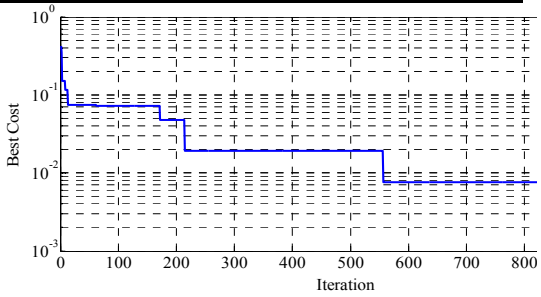

Fig. 6. The convergence rate for STA-TLBO objective function.

Fig. 7 shows the desired and measured position (β) path by applying the PID-TLBO and STA-TLBO controllers in comparison with the STA and PID controllers. As can be seen from Fig. 7, the adjusted coefficients using the TLBO algorithm cause a good performance for the PID-TLBO and STA-TLBO controllers. Also tracking is well done and the tracking error is small.

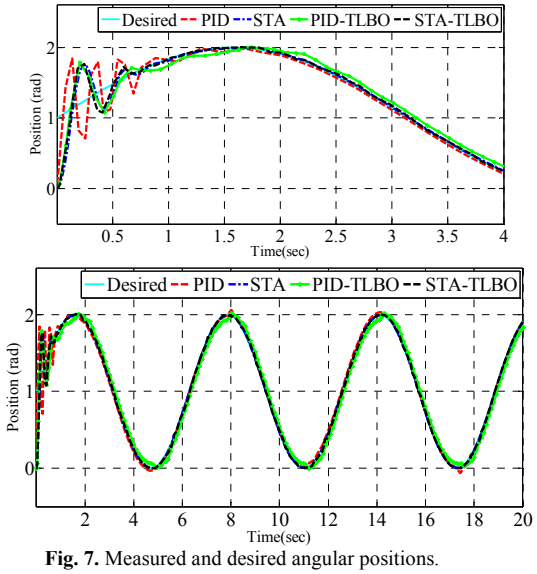

Fig. 7. Measured and desired angular positions.

As can be seen in Fig. 8, the tracking error of PID-TLBO controller is greater than the tracking error of STA-TLBO controller as well as its steady-state error.

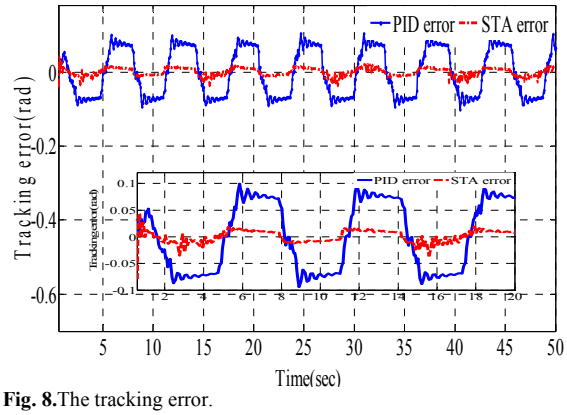

Fig. 8. The tracking error.

5.3. Robustness to external disturbance, and uncertainty

The performance of the designed controller against parametric uncertainty and external disturbance is measured to evaluate its robustness. An external disturbance is applied between 5 and 6 seconds. From Fig. 9, one can see that the proposed controller performs accurate tracking and has limited-time convergence, and is robust despite external perturbations. To investigate the robustness against parameter uncertainty, we changed the parameter values between 5 and 10%. The results can be seen in Fig. 10 and indicate the desired performance of the designed controller.

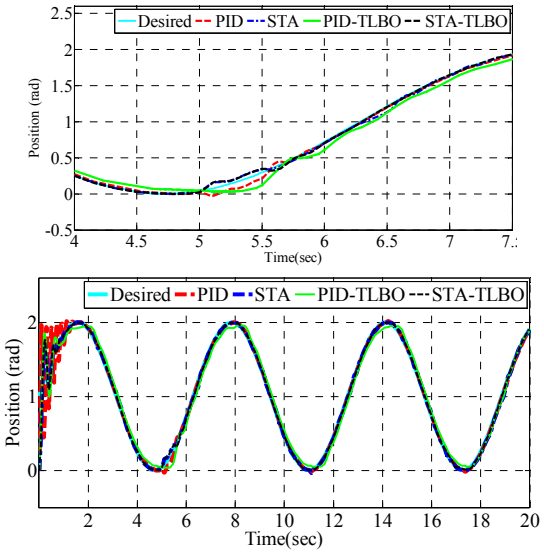

Fig. 9. Measured and desired angular positions under external disturbance.

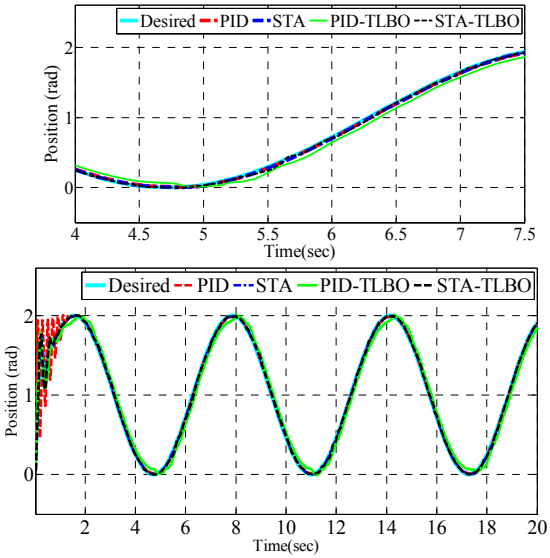

Fig. 10. Measured and desired angular positions under uncertainty.

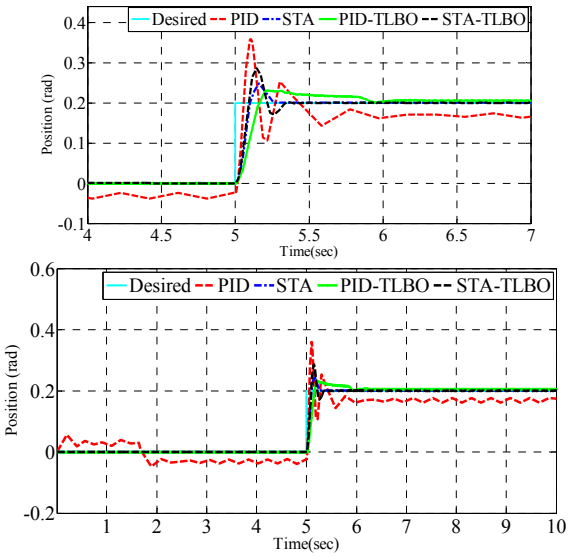

Fig. 11. Step response for the controllers.

5.4. Step response

A step with a value of 0.2 is applied as input to the system in the 5th second. It is easy to see that the adjusted STA controller by the TLBO algorithm has better performance than the other controllers and has a less steady-state error (Fig.11.).

To compare the performance of the controllers, we employed four famous indices, the root-mean-square error (RMS), mean square error (MSE), mean absolute error (MAE), and standard deviation (Sd). The values of mentioned indices are given in Table . It can be seen that the adjusted PID-TLBO and STA-TLBO controllers have smaller tracking errors compared to PID and STA controllers.

Also, the STA-TLBO controller has a better performance than the PID-TLBO controller under the nominal conditions, external disturbances, and step response. Finally, Fig. 12 presents a comprehensive comparison of the performance of the controllers.

6. Conclusion

In this paper, a nonlinear dynamic model of an upper limb robot was developed. A second-order sliding mode controller with a super twisting algorithm is used to control the rehabilitation arm robot. The gains of the STA-TLBO controller are obtained using the TLBO algorithm. To demonstrate the validity of the designed controller, the results are compared to the TLBO-PID, PID, and STA controllers. The superiority of the STA-TLBO controller compared to the others is confirmed by the simulation results.

Table 3. RMS, MSE, MAE, and Sd of controllers.

	Nominal conditions				Parameter uncertainties			
	PID	**STA**	**PID_TLBO**	**STA_TLBO**	**PID**	**STA**	**PID_TLBO**	**STA_TLBO**
RMS	0.1549	0.1174	0.0826	0.0495	0.1052	0.1198	0.0858	0.0903
MSE	0.024	0.0138	0.0068	0.0025	0.0111	0.0143	0.0074	0.0082
MAE	0.0669	0.0216	0.0397	0.0067	0.0261	0.0224	0.0409	0.0163
Sd	0.1397	0.1154	0.0724	0.0491	0.1019	0.1177	0.0754	0.0888
	Disturbances				**Step response**			
	PID	**STA**	**PID_TLBO**	**STA_TLBO**	**PID**	**STA**	**PID_TLBO**	**STA_TLBO**
RMS	0.2042	0.1063	0.0996	0.0965	0.0973	0.0766	0.0124	0.0037
MSE	0.0417	1.13E-02	0.0099	0.0093	0.0095	0.0059	1.53E-04	1.37E-05
MAE	0.0815	0.0219	0.0469	0.0182	0.0672	0.0308	0.0023	1.26E-04
Sd	0.1873	0.104	0.0879	0.0948	0.0704	0.0701	0.0122	0.0037

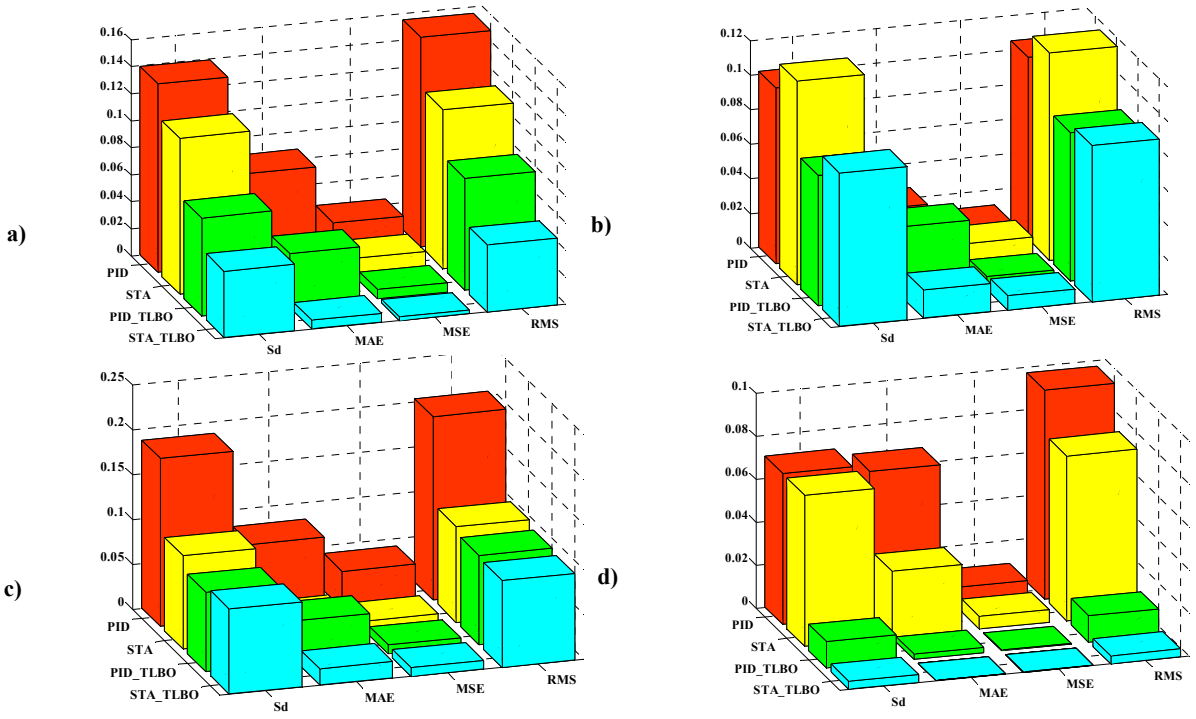

Fig. 12. (a) Nominal conditions; **(b)** Parameter uncertainties; **(c)** Disturbances; **(d)** Step response.

The proposed controller guarantees finite-time convergence, reducing steady-state tracking error, reduced chattering, and stability. The PID-TLBO and STA-TLBO controllers are robust against parameter uncertainties, external disturbances. Also, from the step response, the adjusted controllers with the TLBO algorithm have a more desirable performance in the transient and permanent state. For future works, according to the desired results obtained from the intelligent TLBO algorithm, we can use it to control rehabilitation robots with more degrees of freedom or other rehabilitation robots.

References

1. Zhou, L., Li, Y. and Bai, S., "A human-centered design optimization approach for robotic exoskeletons through biomechanical simulation", *Robotics and Autonomous Systems*, Vol. 91, (2017), 337-347.
2. Asbeck, A.T., De Rossi, S.M., Galiana, I., Ding, Y. and Walsh, C.J., "Stronger, smarter, softer: Next-generation wearable robots", *IEEE Robotics & Automation Magazine*, Vol. 21, No. 4, (2014), 22-33.
3. Lee, S., Crea, S., Malcolm, P., Galiana, I., Asbeck, A. and Walsh, C., "Controlling negative and positive power at the ankle with a soft exosuit", in 2016 IEEE International Conference on Robotics and Automation (ICRA), IEEE., (2016), 3509-3515.
4. Rupal, B.S., Rafique, S., Singla, A., Singla, E., Isaksson, M. and Virk, G.S., "Lower-limb exoskeletons: Research trends and regulatory guidelines in medical and non-medical applications", *International Journal of Advanced Robotic Systems*, Vol. 14, No. 6, (2017), 1729881417743554.
5. Wu, Q., Wang, X., Chen, B. and Wu, H., "Design and fuzzy sliding mode admittance control of a soft wearable exoskeleton for elbow rehabilitation", *IEEE Access*, Vol. 6, (2018), 60249-60263.
6. Villoslada, A., Flores, A., Copaci, D., Blanco, D. and Moreno, L., "High-displacement flexible shape memory alloy actuator for soft wearable robots", *Robotics and Autonomous Systems*, Vol. 73, (2015), 91-101.
7. Nef, T., Mihelj, M. and Riener, R., "Armin: A robot for patient-cooperative arm therapy", *Medical & biological engineering & computing*, Vol. 45, No. 9, (2007), 887-900.
8. Mihelj, M., Nef, T. and Riener, R., "Armin ii-7 dof rehabilitation robot: Mechanics and kinematics", in Proceedings 2007 IEEE

International Conference on Robotics and Automation, IEEE., (2007), 4120-4125.
9. Nef, T., Guidali, M. and Riener, R., "Armin iii–arm therapy exoskeleton with an ergonomic shoulder actuation", *Applied Bionics and Biomechanics*, Vol. 6, No. 2, (2009), 127-142.
10. Stienen, A.H., Hekman, E.E., Prange, G.B., Jannink, M.J., Aalsma, A.M., van der Helm, F.C. and van der Kooij, H., "Dampace: Design of an exoskeleton for force-coordination training in upper-extremity rehabilitation", *Journal of medical devices*, Vol. 3, No. 3, (2009).
11. Otten, A., Voort, C., Stienen, A., Aarts, R., van Asseldonk, E. and van der Kooij, H., "Limpact: A hydraulically powered self-aligning upper limb exoskeleton", *IEEE/ASME transactions on mechatronics*, Vol. 20, No. 5, (2015), 2285-2298.
12. Keller, U., van Hedel, H.J., Klamroth-Marganska, V. and Riener, R., "Charmin: The first actuated exoskeleton robot for pediatric arm rehabilitation", *IEEE/ASME transactions on mechatronics*, Vol. 21, No. 5, (2016), 2201-2213.
13. Brahim, B., Ochoa-Luna, C., Saad, M., Assad-Uz-Zaman, M., Islam, M.R. and Rahman, M.H., "A new adaptive super-twisting control for an exoskeleton robot with dynamic uncertainties", in 2017 IEEE Great Lakes Biomedical Conference (GLBC), IEEE., (2017), 1-1.
14. Stroppa, F., Loconsole, C., Marcheschi, S. and Frisoli, A., A robot-assisted neuro-rehabilitation system for post-stroke patients' motor skill evaluation with alex exoskeleton, in Converging clinical and engineering research on neurorehabilitation ii. 2017, Springer.501-505.
15. Xiao, F., Gao, Y., Wang, Y., Zhu, Y. and Zhao, J., "Design of a wearable cable-driven upper limb exoskeleton based on epicyclic gear trains structure", *Technology and Health Care*, Vol. 25, No. S1, (2017), 3-11.
16. Lu, L., Wu, Q., Chen, X., Shao, Z., Chen, B. and Wu, H., "Development of a semg-based torque estimation control strategy for a soft elbow exoskeleton", *Robotics and Autonomous Systems*, Vol. 111, (2019), 88-98.
17. Kaneko, M., Paetsch, W. and Tolle, H., "Input-dependent stability of joint torque control of tendon-driven robot hands", *IEEE Transactions on Industrial Electronics*, Vol. 39, No. 2, (1992), 96-104.
18. Fuxiang, T. and Xingsong, W., "The design of a tendon-sheath-driven robot", in 2008 15th International Conference on Mechatronics and Machine Vision in Practice, IEEE., (2008), 280-284.
19. Agrawal, V., Peine, W.J., Yao, B. and Choi, S., "Control of cable actuated devices using smooth backlash inverse", in 2010 IEEE International Conference on Robotics and Automation, IEEE., (2010), 1074-1079.
20. Dinh, B.K., Xiloyannis, M., Cappello, L., Antuvan, C.W., Yen, S.-C. and Masia, L., "Adaptive backlash compensation in upper limb soft wearable exoskeletons", *Robotics and Autonomous Systems*, Vol. 92, (2017), 173-186.
21. Falisse, A., Van Rossom, S., Jonkers, I. and De Groote, F., "Emg-driven optimal estimation of subject-specific hill model muscle–tendon parameters of the knee joint actuators", *IEEE Transactions on Biomedical Engineering*, Vol. 64, No. 9, (2016), 2253-2262.
22. Crea, S., Cempini, M., Moise, M., Baldoni, A., Trigili, E., Marconi, D., Cortese, M., Giovacchini, F., Posteraro, F. and Vitiello, N., "A novel shoulder-elbow exoskeleton with series elastic actuators", in 2016 6th IEEE International Conference on Biomedical Robotics and Biomechatronics (BioRob), IEEE., (2016), 1248-1253.
23. Kawasaki, H., Ito, S., Ishigure, Y., Nishimoto, Y., Aoki, T., Mouri, T., Sakaeda, H. and Abe, M., "Development of a hand motion assist robot for rehabilitation therapy by patient self-motion control", in 2007 IEEE 10th International Conference on Rehabilitation Robotics, IEEE., (2007), 234-240.
24. Rosati, G., Gallina, P. and Masiero, S., "Design, implementation and clinical tests of a wire-based robot for neurorehabilitation", *IEEE Transactions on Neural Systems and Rehabilitation Engineering*, Vol. 15, No. 4, (2007), 560-569.
25. Sharma, M.K. and Ordonez, R., "Design and fabrication of an intention based upper-limb exo-skeleton", in 2016 IEEE International Symposium on Intelligent Control (ISIC), IEEE., (2016), 1-6.
26. Li, L., Weng, W. and Fujimura, S., "An improved teaching-learning-based optimization algorithm to solve job shop scheduling problems", in 2017 IEEE/ACIS 16th International Conference on Computer

and Information Science (ICIS), IEEE., (2017), 797-801.
27. Kiguchi, K., Tanaka, T. and Fukuda, T., "Neuro-fuzzy control of a robotic exoskeleton with emg signals", *IEEE Transactions on fuzzy systems*, Vol. 12, No. 4, (2004), 481-490.
28. Kang, H.-B. and Wang, J.-H., "Adaptive robust control of 5 dof upper-limb exoskeleton robot", *International Journal of Control, Automation and Systems*, Vol. 13, No. 3, (2015), 733-741.
29. Rahman, M.H., Saad, M., Kenné, J.P. and Archambault, P.S., "Nonlinear sliding mode control implementation of an upper limb exoskeleton robot to provide passive rehabilitation therapy", in International Conference on Intelligent Robotics and Applications, Springer., (2012), 52-62.
30. Lilly, J.H. and Quesada, P.M., "A two-input sliding-mode controller for a planar arm actuated by four pneumatic muscle groups", *IEEE Transactions on Neural Systems and Rehabilitation Engineering*, Vol. 12, No. 3, (2004), 349-359.
31. Rahman, M., Saad, M., Kenne, J. and Archambault, P., "Modeling and development of an exoskeleton robot for rehabilitation of wrist movements", in 2010 IEEE/ASME International Conference on Advanced Intelligent Mechatronics, IEEE., (2010), 25-30.
32. Rahman, M.H., Kittel-Ouimet, T., Saad, M., Kenné, J.-P. and Archambault, P.S., "Development and control of a robotic exoskeleton for shoulder, elbow and forearm movement assistance", *Applied Bionics and Biomechanics*, Vol. 9, No. 3, (2012), 275-292.
33. Joo, Y.H. and Duong, P.X., "Parameter estimator integrated-sliding mode control of dual arm robots", *International Journal of Control, Automation and Systems*, Vol. 15, No. 6, (2017), 2754-2763.
34. Ali Akbar Semnani, M., Vali, A., Hakimi, S.M. and behnamgol, v., "Heartbeat ecg tracking systems using observer based nonlinear controller", *Journal of Applied Dynamic Systems and Control*, Vol. 4, No. 2, (2021), 69-78.
35. Hokmabadi, A., "Study and design of a fractional-order terminal sliding mode fault-tolerant control for spacecraft", *Journal of Applied Dynamic Systems and Control*, Vol. 1, No. 1, (2018), 10-15.
36. Rao, R.V., Savsani, V.J. and Vakharia, D., "Teaching–learning-based optimization: A novel method for constrained mechanical design optimization problems", *Computer-Aided Design*, Vol. 43, No. 3, (2011), 303-315.
37. Niknam, T., Azizipanah-Abarghooee, R. and Narimani, M.R., "A new multi objective optimization approach based on tlbo for location of automatic voltage regulators in distribution systems", *Engineering Applications of Artificial Intelligence*, Vol. 25, No. 8, (2012), 1577-1588.
38. Rao, R.V., Savsani, V.J. and Vakharia, D., "Teaching–learning-based optimization: An optimization method for continuous non-linear large scale problems", *Information sciences*, Vol. 183, No. 1, (2012), 1-15.
39. Rosales, Y., Lopez, R., Rosales, I., Salazar, S. and Lozano, R., "Design and modeling of an upper limb exoskeleton", in 2015 19th International Conference on System Theory, Control and Computing (ICSTCC), IEEE. Vol., No. Issue, (2015), 266-272.
40. Mirrashid, N., Alibeiki, E. and Rakhtala, S.M., "Development and control of an upper limb rehabilitation robot via aco-pid and fuzzy-pid controllers", *International Journal of Engineering*, Vol. 35, No. 8, (2022), -.
41. Mirrashid, N., Alibeiki, E. and Rakhtala, S.M., "Nonlinear robust controller design for an upper limb rehabilitation robot via variable gain super twisting sliding mode", *International Journal of Dynamics and Control*, (2022).
42. Fazli, E., Rakhtala, S.M., Mirrashid, N. and Karimi, H.R., "Real-time implementation of a super twisting control algorithm for an upper limb wearable robot", *Mechatronics*, Vol. 84, (2022), 102808.
43. Levant, A., "Sliding order and sliding accuracy in sliding mode control", *International journal of control*, Vol. 58, No. 6, (1993), 1247-1263.
44. Mirrashid, N., Rakhtala, S.M. and Ghanbari, M., "Robust control design for air breathing proton exchange membrane fuel cell system via variable gain second-order sliding mode", *Energy Science & Engineering*, Vol. 6, No. 3, (2018), 126-143.